Research Article

Intelligent Tomographic Microwave Imaging for Breast Tumor Localization

Ibrahim M. Mehedi [ID],[1,2] **K. Prahlad Rao,**[1] **Ubaid M. Al-Saggaf** [ID],[1,2]
Hadi Mohsen Alkanfery,[1] **Maamar Bettayeb,**[2,3] **and Rahtul Jannat** [ID][4]

[1]*Department of Electrical and Computer Engineering (ECE), King Abdulaziz University, Jeddah 21589, Saudi Arabia*
[2]*Center of Excellence in Intelligent Engineering Systems (CEIES), King Abdulaziz University, Jeddah 21589, Saudi Arabia*
[3]*Electrical & Computer Engineering Department, University of Sharjah, Sharjah, UAE*
[4]*Department of Electrical and Electronic Engineering, BRAC University, Dhaka, Bangladesh*

Correspondence should be addressed to Rahtul Jannat; mrahatuljannat@gmail.com

Researchers are continuously exploring the potential use of microwave imaging in the early detection of breast cancer. The technique offers a promising alternative to mammography, a standard clinical imaging procedure today. The contrast in dielectric properties between normal and cancerous tissues makes microwave imaging a viable technique for detecting breast cancer. Experimental results are presented in this paper that demonstrate the detection of breast cancer using microwaves operating at 2.4 GHz. The procedure involves antenna fabrication, phantom tissue development, and image reconstruction. Design and fabrication of patch antenna are used in the study, described in detail. The patch antenna pair is used for transmitting and receiving source waves. Tissue mimicking models were developed from paraffin wax and glycerin for the dielectric constants of 9 and 47, respectively, representing the tissue and tumor. Further, AI-based tomographic images were obtained by implementing a filtered back-projection algorithm in the computer. In the results, the presence of the tumor is quantitatively analyzed.

1. Introduction

Hippocrates, the father of medicine, described cancer as one of the oldest deadly diseases in the ancient world. Breast cancer is the most life-threatening severe disease among women, second only to liver cancer as the leading cause of death [2]. Breast cancer survivorship rates improve when women undergo annual screenings to detect cancerous tumors and receive appropriate treatment. Screening techniques include X-ray mammography, ultrasound, and magnetic resonance imaging (MRI). Both have advantages and limitations. Ionizing radiation is hazardous to biological tissue. Furthermore, tumor detection rates are lower in dense breasts [3]. Ultrasound is a low-cost method, but its effectiveness depends on the operators' expertise [4]. Breast images produced by MRI can be highly detailed. However, it is too costly for normal screening usage [5]. A microwave-based imaging system is an attractive substitute or complement modality to the existing methods since it has the benefits mentioned above in breast imaging. It is possible to get high-resolution breast images with microwave transmitters without ionizing tissue. In addition, current microwave technology allows for the development of highly efficient, compact, and fully automated systems that apply to a wide range of applications and minimize the possibility of human error. Numerous studies have used microwave breast imaging techniques [6–10]. The main similarities among these systems are the infrastructure and the algorithm used to reconstruct the images. There are ultra-wideband (UWB) antennas covering a wide frequency range, but they have a tradeoff between loss of power and the ability to penetrate the tissue. Saturation media such as saline or glycerol can improve the coupling between antennas by reducing mismatches at their interface with the skin. Additionally, breast

anatomy is typically visualized by tomographic or radar-based analysis methods, such as the Gauss–Newton method [11], delay and sum (DAS) [12], or microwave space-time beamforming (MIST) [13].

Clinicians and researchers are trying to save the lives of patients through early diagnosis and effective treatment procedures. Suppose the cancer is detected in its early stages through periodic breast screening, and the survival rate of women increases. Apart from pathological tests, diagnostic imaging plays a crucial role in the early detection of breast cancer. Imaging involves characterizing a signal and separating it from the background. To characterize the tissues in medical imaging applications, a variety of sources have been used—controlled propagation of X-rays from X-ray tubes that provide an image of internal body parts for diagnosis. The X-ray particles passed through the body are recorded in the form of an image. Magnetic resonance images are produced by using a magnetic field and radio waves. They offer higher resolution with excellent contrast to the tissue. Powerful magnets are used to produce the field and the radiofrequency pulses obtained from r.f. coils. The scans of cross sections of internal body organs generated from projections can detect the slightest change in physiological or anatomical changes in the body parts. Relatively inexpensive ultrasound scanners use high-frequency sound waves to diagnose and treat patients. The pulses of sound waves generated from a piezoelectric crystal are transmitted and received from the ultrasound transmitter through tissues. The received signals are processed to display the characterized values of the tissue as its image. These three techniques are implemented in commonly used imaging modalities in hospitals. However, there are a few concerns about these systems, such as ionizing radiation, cost, size, portability, complicated instrumentation, and scary among the patients undergoing scanning. Presently, mammography [15] is being used as a standard screening method for breast cancer detection that uses X-ray radiations to characterize the dense masses present in breast tissue. There are shreds of evidence that the mammogram images failed to detect suspicious lesions present in the breast. Sensitivity and specificity are the limiting values that make this imaging method restricted to a false-positive rate of 4%–34% [16]. A false-negative rate could be as high as 70% [17]. Therefore, X-ray mammography is not entirely safe for repeated screening and cannot be considered a single stand-alone test for breast cancer diagnosis. Magnetic resonance imaging (MRI) is more promising for breast imaging which can detect cancers in dense breasts that are failed to detect in mammograms. Images obtained from MRI machines are superior insensitivity that sometimes makes suspicious tissue as tumors wrongly resulting in a high rate of false positive [18].

In detecting benign and malignant tissues, two different contrast agents are used. When the uptake is tracked for individual contrast agents, the results from scans will become more complex while interpreting the images. Usually, breast MRI is not followed as a routine screening method for cancer diagnosis, but they are recommended only for women at high risk. The logistic facility, procurement of MRI scanners, and cost limit their use in hospitals. Ultrasound can distinguish between a liquid-filled cyst and a dense solid mass. However, it is not used for early stage cancer detection; instead, ultrasound is often used as a follow-up test after mammography or MRI detects the tumor. All these three prominent breast imaging techniques sometimes show a false-positive result. Microwave-based imaging techniques have been attracted by researchers for detecting breast cancer at an early stage due to their merits of safety, high contrast, less expensive, no discomfort to the patients during the examination, and relatively more minor complexity in instrumentation. Microwaves are radio waves that are a part of electromagnetic radiation in the frequency range of 300 MHz (100 cm)–300 GHz (0.1 cm), used in telecommunications, radar, domestic heating appliances, food, and medical applications. Images for medical purposes at microwave frequency are the spatial distribution of electrical parameters of the body. Instead of showing tissue structures, these images show the two-dimensional distribution of electromagnetic properties. Because healthy and fat tissue is translucent at microwave frequencies, microwave imaging can be used in the early detection of breast cancer by comparing the contrast values of electrical properties between normal and cancerous tissues [19, 20].

Several researchers have reported microwave imaging techniques for various applications with different terminologies and algorithms, including nondestructing testing, detection of weapons in the military, security checks at public places for prohibitive measures, monitoring of civil structures' life, and see-through imaging. The methodology of imaging at microwave frequencies has been reported as radar-based imaging [21–23]. Compared to the gold standard MRI [24], ultrasound [25], and X-ray-based mammography [26] diagnostic screening methods, microwave imaging can characterize the tumor in terms of dielectric constant rather than characterizing as dense tissue [27]. Hardware for microwave imaging requires an antenna that transmits microwave energy penetrating the breast tissue, and a receiver receives the signal. The received signal carries information about the object through which it propagated. A computer creates a two-dimensional digital map of the object based on the contrast values of electrical parameters. A phantom study demonstrates instrumentation for detecting tumors in tissue. Using the filtered back-projected image reconstruction algorithm [28], a cross-sectional image of the tumor is reconstructed.

2. Methodology

Microwave Tomography and Materials Research Laboratory was the laboratory that carried out the study. Samples of breast tissue for the study were obtained from the Department of Surgery within 30 minutes following a mastectomy. Microwave imaging is a noninvasive technique for observing the internal structure of the body organs through electromagnetic fields. When the short-duration pulses of low-energy microwaves travel and shine on the breast tissue from a transmitting antenna, the reflections are collected by a receiver antenna, and they are further processed to create

an image that gives inside information about the tissue. The sketch shown in Figure 1 represents the principle of microwave imaging. The transmitted waves scatter in the biological tissue due to the presence of a target. The electrical properties of the tissue govern the interaction of tissue with electromagnetic waves. Some of the typical electrical properties of any material in biomedical applications dealing with electromagnetic energy are specified by conductivity, dielectric permittivity, and the loss component. The conductivity of the biological tissue changes from one person to another due to their complex physiological conditions [29, 30]. It is remarkable how little dielectric loss the breast has [31]. Thus, the dielectric permittivity is assumed to greatly affect tissue scattering due to electromagnetic waves. By measuring scattered waves as a function of dielectric permittivity, a two-dimensional map can be created. The hardware required for microwave imaging of breast tumors has three main parts; transmission of microwave energy, receiving the signal, and processing the signal to obtain images of dielectric constant (ε) that illustrate the tumor present in breast tissue.

2.1. Microwave Transmitting Antenna.
Microwaves are electromagnetic waves often referred to as radio waves in the range of 300 MHz to 300 GHz. A small portion of the frequency band over the radio spectrum is exclusively reserved internationally for industrial, scientific, and medical applications other than commercial telecommunication applications [32]. The ISM frequency band free from operating licenses is clustered around 2.4 GHz and 900 MHz. The radio waves are transmitted or received by a device known as an antenna. The microwave antennas are available in microstrip patch, horn, parabolic, plasma, and MIMO (multiple input multiple output) antennas. Microstrip patch antennas are preferred over conventional antennas for biomedical applications due to their low profile, small size, narrow bandwidth, easy customization, simple fabrication steps, and low cost. In the study of breast cancer detection, two patch antennas are designed and fabricated for operating in the ISM band of frequency (2.4 GHz).

2.2. Microstrip Patch Antenna Design.
Since our interest is to employ the antenna in imaging applications for medical diagnosis, we chose a more compact and straightforward rectangle structure than any complex geometries. Therefore, the dimensions are calculated from the below given equations [33].

The width of the patch is known from

$$W = \frac{C_0}{2f_r} \sqrt{\frac{2}{\varepsilon_r + 1}}, \qquad (1)$$

where W = width; C_0 = speed of light; ε_r = dielectric constant of substrate; and f_r = resonance frequency.

Length is given by

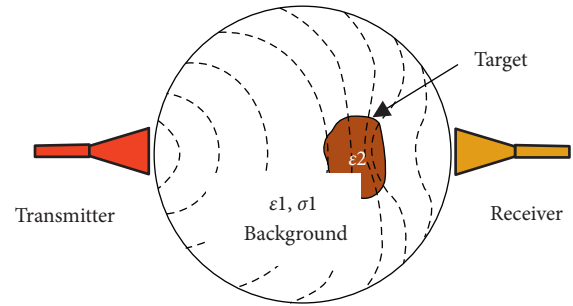$$L = \frac{C_0}{2f_r \sqrt{\varepsilon_{\text{reff}}}} - 2(\Delta L), \qquad (2)$$

FIGURE 1: Principle of microwave imaging.

where L = length of the patch; (ΔL) = increase in length due to fringing effect; and $\varepsilon_{\text{reff}}$ is the effective dielectric constant known from

$$\varepsilon_{\text{reff}} = \frac{\varepsilon_r + 1}{2} + \frac{\varepsilon_r - 1}{2}\left(1 + 12\frac{h}{2}\right)^{-1/2}, \text{ but } \frac{w}{h} > 1, \qquad (3)$$

where h = height of the substrate.

The patch antenna consists of three layers. The top layer is the patch, below which a substrate is laid, and the bottom layer has a ground plane.

The feed line impedance is 50 Ohms, but the radiation resistance at its edge is much better than the feed line impedance, resulting in a mismatch. Using an inset feed technique, the antenna's performance is improved by reducing reflections in order to achieve maximum power transfer. It is estimated that the antenna feed edge matches the transmission line's characteristic impedance by the distance of inset feeding. The optimal value of the inset feed is 12 mm in our design.

2.3. Simulation.
From the design equations given above, both L and W dimensions are obtained as 29.2 mm for the resonating frequency of 2.4 GHz. The microstrip patch antenna is simulated in CST Microwave Studio (Computer Simulation Technology) software. The substrate FR4 is readily available and commonly used in making PCBs (printed circuit boards), with $\varepsilon_r = 4.4$ being used in the simulation. Figure 2 shows the structure and field distribution of the antenna, and Figure 3 illustrates the layout obtained from the simulation software. Figure 4 shows the configuration of the sandwiched patch, substrate, and ground plane together, thus making a patch antenna. Figure 5 shows antenna parameters plotted against frequency. It can be noted that the gain at the resonant frequency is 5.834 dB and the directivity at the same frequency is 5.830 dB. The fitted value of return loss (S11) is −26 dB, shown in Figure 6.

2.4. Fabrication.
After estimating the physical dimensions and running simulation software, our laboratory fabricated the proposed antenna from LPKF Laser and Electronics PCB milling station. Since it is easier to fabricate and costs less, the FR4 material was used for the antenna. The milling station works with a laser source that removes copper from
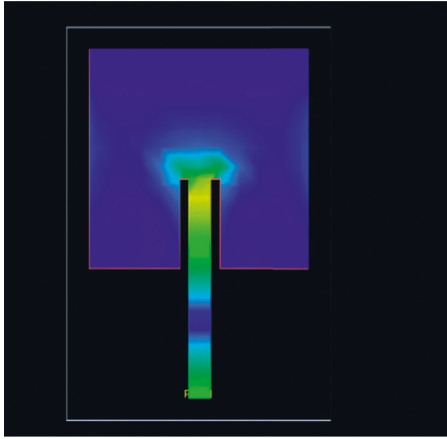
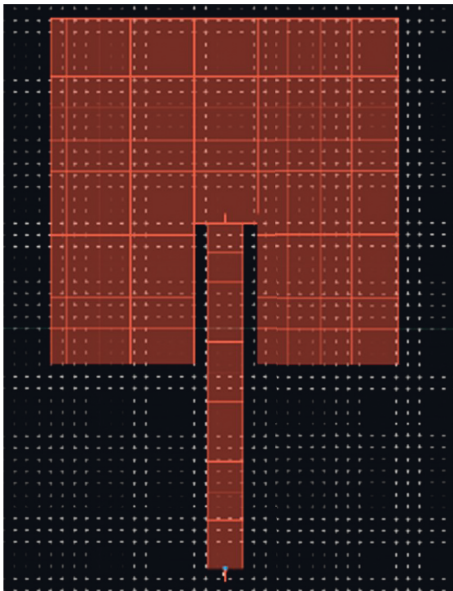FIGURE 2: Structure and field distribution.

FIGURE 3: The layout of the patch antenna.

the substrate and precisely leaves behind a pattern. The Gerber file generated from the simulation is exported to the machine, and then, the cleaned substrate sheet is positioned inside the machine's hood. Initial settings of the laser power, nozzle distance, and other necessary values of the machine were adjusted suitably for printing on the substrate. After completion of etching, the antenna was removed and cleaned again to remove the dirt and etched out copper particles from the substrate. For feeding the antenna, the coaxial feed technique was used in which an SMA port was soldered carefully at the specified transmission line feed input position, and the connection was established carefully between the port and the microstrip feed line. Figure 7 shows the photograph of the antenna with the feed line connector. In Figure 6, the dB return loss (S11) is shown for simulated and measured values. The comparison indicates that the return loss value by simulation is −25 dB, and the same by measurements is −20 dB. The values exactly do not match the 2.4 GHz frequency, but they are very close to the resonant frequency.

In the final stage, the performance of the fabricated antenna was experimentally verified by measuring the return loss characteristics from a Vector Network Analyzer (Agilent Technologies, N5230 A). Before measurements, the VNA was calibrated, the antenna was tested, and the readings were plotted on a graph as shown in Figure 6. It is noted that the simulated and measured values match each other with minor deviations at the frequency point. However, the S11 values are slightly shifted from the desired resonant frequency. It is believed that the difference could be due to the placement and soldering of the port and cutting away the fabricated antenna from the FR4 dielectric sheet.

2.5. Breast Phantom. A phantom is a realistic model representing an actual object and is often used to evaluate new techniques or algorithms in terms of their potential and limitations and standardize the technique developed. Breast phantoms were used in our experiment to test the potential of breast cancer detection by tomographic imaging using microwaves. FBP algorithm has been implemented to produce the slice image of the solid tissue phantom. Several methods of the phantom for breast have been reported using soybean oil [34, 35], polyacrylamide [36], Vaseline cream and wheat flour [37], and oil with polypropylene [38] and glycerin with water mixture [39]. However, most of them do not have ideal phantom characteristics. A phantom is ideal if it is homogeneous, solid, stable over a long period, allows easy tuning of electrical properties, is moldable to the desired shape, and is inexpensive. Most of the phantoms mentioned are liquids, which do not allow uniform distribution of scattering particles within the medium and therefore are not homogeneous and are not stable over a long period.

To overcome the difficulties associated with liquid phantoms, solid tissue-equivalent phantoms using paraffin wax were developed and used. The wax is a natural product derived from the molecular components of decayed vegetable and animal material. It consists of a complex mixture of hydrocarbons. It is colorless and nonreactive, and can be cast easily with uniform mixing of coloring materials. At ambient temperature, the wax remains solid, starts melting when the temperature exceeds 37°C, and starts to boil when the temperature rises to 370°C. Because of this thermal property, the wax can be easily moldable to any shape. It is a perfect electrical insulator having electrical resistivity greater than 7.92×10^7 Ohm-cm, and the dielectric constant decreases monotonically as a function of frequency in the microwave band of frequency [40]. In the microwave band of frequencies up to 5 GHz, the dielectric constant of the wax is reported in the range of 2–7 [41]. There is a remarkable contrast between the normal breast tissue and tumor in the dielectric constant value [42]. Several researchers have published electrical properties of biological tissues from their extensive works [6, 43–51]. From these references, the dielectric constants of fatty tissue and the tumor are 9 and 47, respectively. Since the dielectric value of the normal breast tissue matches that of the wax, we used the plain paraffin wax to develop the breast phantom.
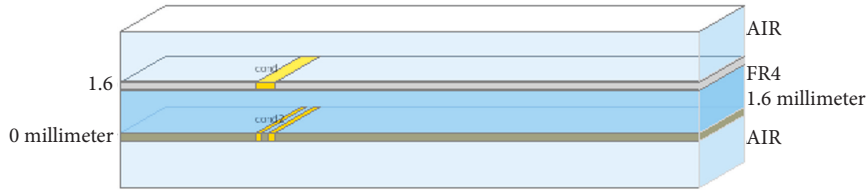
FIGURE 4: Configuration of the sandwiched ground plate, substrate, and patch layers.
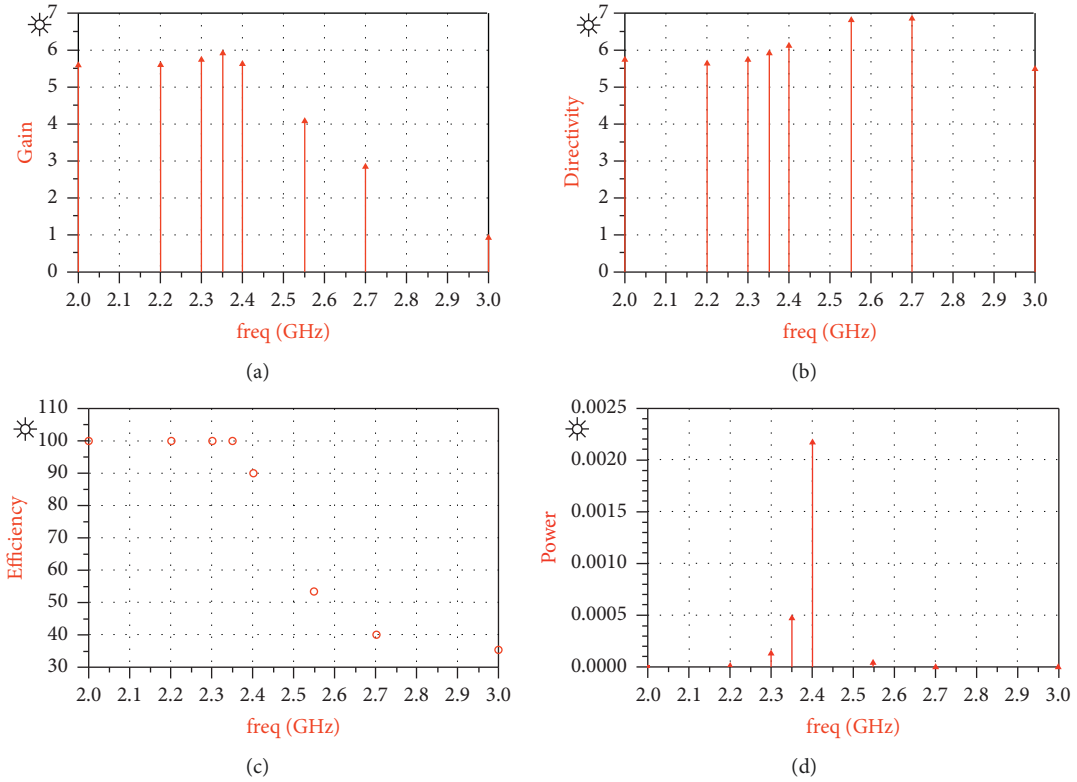

(a)

(b)

(c)

(d)

FIGURE 5: Antenna parameters obtained from simulation. The parameters gain, directivity, efficiency, and rated power are plotted against frequency. (a) Gain (dBi). (b) Directivity (dBi). (c) Efficiency (%). (d) Power radiated (watts).
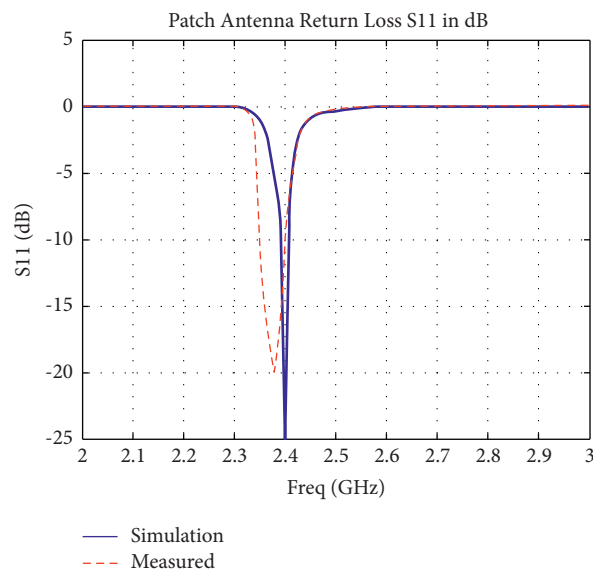

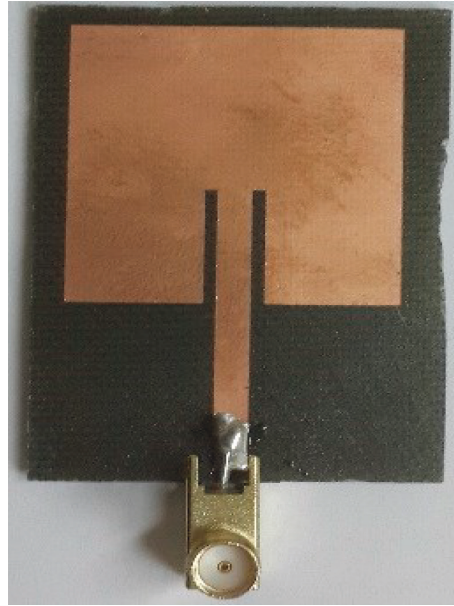FIGURE 6: Results of S11 (dB) from simulation and measurements.

Figure 7: Photograph of fabricated patch antenna.

The wax was heated at a steady and low temperature and allowed to change from solid to liquid state. Then, it was poured into a mold to make a cylindrical-shaped phantom. The diameter of the cylinder was measured at 80 mm and the height at 80 mm. After cooling entirely at room temperature, the cylindrical-shaped phantom of the desired dimension was obtained. To mimic the tumor, a hole of 10 mm diameter was carefully drilled axially at the center of the wax cylinder, and it was filled with the mixture of glycerin-water (80 : 20%). Glycerin is a nontoxic, colorless viscous liquid, a polyol compound widely used in the food industry and pharmaceutical combinations. The dielectric constant of the glycerin at room temperature is 47 [52], which is a close match with the tumor dielectric constant. The stable and homogeneous breast tissue phantom inclusive of contrast anomaly mimicking tumor was fabricated referring to reported typical values of electrical properties. The phantom was then used in our experiment of AI-based tomographic imaging at the ISM frequency range.

2.6. AI-Based Tomographic Image Reconstruction. Tomography is an imaging technique for generating a lateral view of an object when a suitable energy source passes through it. The technique is popularly used in X-ray CT scanning (computed tomography), in which X-ray waves are passed through the tissue for medical diagnostic applications. Tomogram is produced in the computer through several algorithms. In this work, the tomographic image of breast tissue phantom is obtained by the filtered back-projection (FBP) algorithm, which is measurement-based rather than a model-based technique such as the iterative method. When the source antenna transmits (Tx) microwaves passing through the tissue, the signal on the opposite side is received by a receiving antenna (Rx). An impulse

generator is used and set to produce a microwave at a 2.4 GHz frequency. Figure 8 shows the experimental setup in which the pair of Tx and Rx is rotated around the tissue phantom to acquire the projections, representing the tumor in terms of differential values of dielectric constants. The phantom, placed on a rotating table, is rotated at 10° step intervals. The signal is measured from VNA and stored in the computer at each step. The computer produces an image by back-projecting the measured values onto the image plane. Because of this, the method is known as back-projection. This image is approximately the same as that of the original object. In this process, the image gets blurred due to artifacts. Using a high-pass filter eliminates the blurring, which is realized through a ramp filter [53]. Hence, the combined back-projection and ramp filtering method is popularly known as filtered back-projection. In this work, signal processing and image reconstruction have been implemented on the computer with MATLAB software programming. In this algorithm, the projections are expressed as Radon transform of the object, which is defined as

$$P_\theta(t) = \int_{(\theta,t)\text{line}} f(x, y)\text{ds}. \tag{4}$$

The above equation can be written using a delta function as

$$P_\theta(t) = \int_{-\infty}^{\infty} \int_{-\infty}^{\infty} f(x, y)[\delta(x\cos(\theta) + y\sin(\theta) - t)t\text{dxdy}], \tag{5}$$

i.e., the line integral along a line of parallel beam rotated at an angle θ from the origin. A set of these functions for constant angle are the projections of the object at the cross section where the rays are being passed. The angle θ is held constant throughout the projection to obtain parallel projection data.
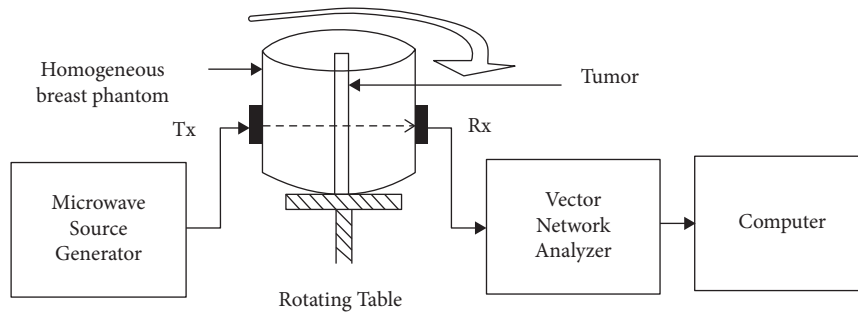
FIGURE 8: An experimental set of microwave imaging for the detection of breast tumor.
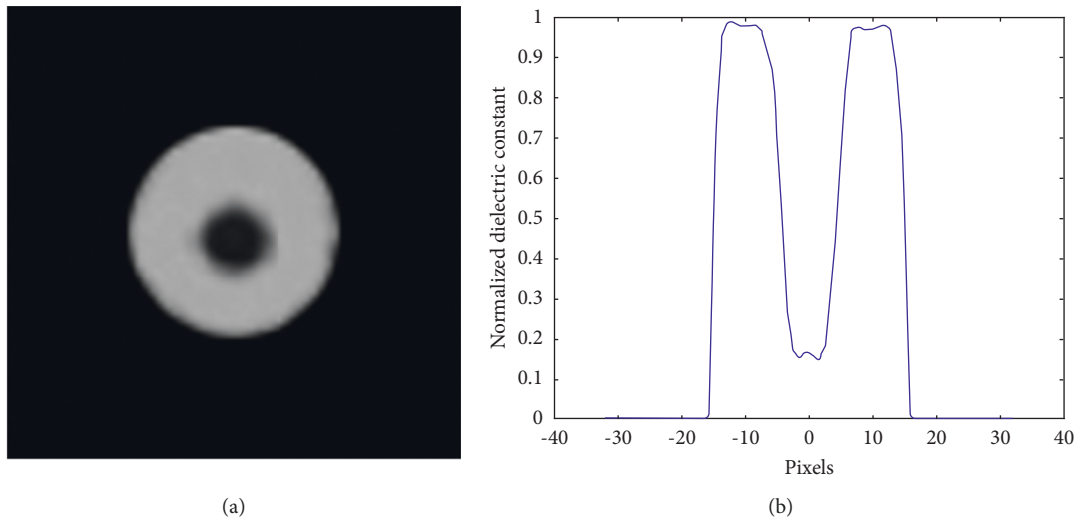

(a)

(b)

FIGURE 9: (a) Reconstructed image of the tissue phantom, including abnormality in the center. (b) The line plot of the normalized dielectric vs. pixels through the center.

3. Results and Discussion

The imaging potential of the developed system for breast cancer detection from microwaves was tested on an indigenously fabricated paraffin wax phantom. The phantom was cylindrical with 80 mm in diameter and 80 mm in height. Figure 9 shows the image of the phantom with abnormality included in the center. A Gaussian filter smoothened the image. The line plot of the image in Figure 9(b) shows the normalized dielectric variation through the center of the image. The decreased dielectric value in the center of the plot indicates the presence of abnormality in the fatty breast tissue.

4. Conclusions

We have developed a setup for breast cancer detection and demonstrated the potential of microwaves for imaging tumor localization. Due to inexpensive hardware, relatively no complexity in instrumentation, easy to fabricate, and harmless for repeated screening, the system could be used as an adjunct to the standard X-ray mammography in diagnosing breast cancer patients. The energy source used is a microwave in the ISM range of frequency that does arise licensing from authorities. To transmit and receive this energy, pair of geometrically simpler rectangular patch antennas were designed, simulated, and fabricated. For the desired frequency of 2.4 GHz on an optimal patch size of 29.2 mm × 29.2 mm with an inset-fed patch antenna, the −25 dB return loss and 5.834 dB gain were obtained. A standard FR4 dielectric material sheet of 1.6 mm thick was used for fabricating the antenna. The measured performance readings were found to agree with the simulated values. The phantoms were made from paraffin wax with dimensions of 80 mm in diameter and 80 mm high. The axial hole was made with a diameter of 10 mm and filled with glycerin-water mixture to simulate a breast tumor. For the cross-sectional images, these phantoms were used. To reconstruct tomographic images, the filtered back-projection algorithm was implemented on a computer using MATLAB software. Using the FBP program, 2-D images of the phantoms were obtained. Through a plot of the profile of the reconstructed image, we were able to see the inclusion of 10 mm diameter fat in the breast tissue.

Data Availability

This article includes all available data.

Conflicts of Interest

Acknowledgments

References

[1] S. Albert, *Microstrip Antenna Arrays, Microstrip Antennas*, P. Nasimuddin, Ed., IntechOpen, London, UK, 2011.

[2] M. S. S. Alwan and Z. Katbay, "Investigation of tumor using an antenna scanning system," *IEEE Microwave Symp*, vol. 171, pp. 1401–1406, 2014.

[3] J. Kissane, J. A. Neutze, H. Singh, and S. Patel, *Radiology Fundamentals Introduction to Imaging and Technology*, Springer, Cham, Switzerland, 6th edition, 2020.

[4] A. N. Sencha, E. V. Evseeva, M. S. Mogutov, and Y. N. Patrunov, *Breast Ultrasound*, Springer, Berlin, Germany, 2014.

[5] R. E. Hendrick, *Breast MRI: Fundamentals and Technical Aspects*, Springer, New York, NY, USA, 2007.

[6] P. M. Meaney, M. W. Fanning, D. Li, S. P. Poplack, and K. D. Paulsen, "A clinical prototype for active microwave imaging of the breast," *IEEE Transactions on Microwave Theory and Techniques*, vol. 48, no. 11, pp. 1841–1853, Nov. 2000.

[7] E. C. Fear, J. Bourqui, C. Curtis, D. Mew, B. Docktor, and C. Romano, "Microwave breast imaging with a monostatic radar-based system: a study of application to patients," *IEEE Transactions on Microwave Theory and Techniques*, vol. 61, no. 5, pp. 2119–2128, May 2013.

[8] A. W. Preece, I. Craddock, M. Shere, L. Jones, and H. L. Winton, "Maria M4: clinical evaluation of a prototype ultrawideband radar scanner for breast cancer detection," *Journal of Medical Imaging*, vol. 3, no. 3, Article ID 033502, Jul. 2016.

[9] E. Porter, M. Coates, and M. Popovic, "An early clinical study of ´ time-domain microwave radar for breast health monitoring," *IEEE Transactions on Biomedical Engineering*, vol. 63, no. 3, pp. 530–539, Mar. 2016.

[10] H. Song, S. Sasada, T. Kadoya et al., "Detectability of breast tumor by a hand-held impulseradar detector: performance evaluation and pilot clinical study," *Scientific Reports*, vol. 7, no. 1, Art. no. 16353, Dec. 2017.

[11] T. M. Grzegorczyk, P. M. Meaney, P. A. Kaufman, R. M. di Florio-Alexander, and K. D. Paulsen, "Fast 3-D tomographic microwave imaging for breast cancer detection," *IEEE Transactions on Medical Imaging*, vol. 31, no. 8, pp. 1584–1592, Aug. 2012.

[12] J. M. Ortega and W. C. Rheinboldt, *Iterative Solution of Nonlinear Equations in Several Variables (Classics in Applied Mathematics)*, Soc Ind Appl Math, Philadelphia. PA, USA, 1970.

[13] R. Benjamin, "Synthetic, post-reception focusing in near-field radar," in *Proceedings of the Proc. EUREL Int. Conf. Detection Abandoned Land Mines Humanitarian Imperative Seeking Tech. Solution*, pp. 133–137, Edinburgh, UK, October 1996.

[14] A. H. Golnabi, P. M. Meaney, and K. D. Paulsen, "3D microwave tomography of the breast using prior anatomical information," *Medical Physics*, vol. 43, no. 4, pp. 1933–1944, 2016.

[15] D. Andreuccetti, M. Bini, A. Ignesti, R. Olmi, N. Rubino, and R. Vanni, "Use of polyacrylamide as a tissue-equivalent material in the microwave range," *IEEE Transactions on Biomedical Engineering*, vol. 35, no. 4, pp. 275–277, 1988.

[16] M. H. Bah, J. S. Hong, and D. A. Jamro, "Study of breast tissues dielectric properties in UWB range for microwave breast cancer imaging," in *Proceedings of the International Conference on Computer Information Systems and Industrial Applications*, pp. 473–475, Bangkok, Thailand, January 2015.

[17] F. Bray, P. McCarron, and D. M. Parkin, "The changing global patterns of female breast cancer incidence and mortality," *Breast Cancer Research*, vol. 6, no. 6, pp. 229–239, 2004.

[18] J. W. Black, "X-ray diagnosis of diseases of the breast [abridged]," *Proceedings of the Royal Society of Medicine*, vol. 56, no. 9, pp. 767–770, 1963.

[19] S. Brovoll, T. Berger, Y. Paichard et al., "Time-lapse imaging of human heart motion with switched array uwb radar," *IEEE Transactions on Biomedical Circuits and Systems*, vol. 8, no. 5, pp. 704–715, 2014.

[20] S. S. Chaudhary, R. K. Mishra, A. Swarup, and J. M. Thomas, "Dielectric properties of normal & malignant human breast tissues at radiowave & microwave frequencies," *Indian Journal of Biochemistry & Biophysics*, vol. 21, pp. 76–79, 1984.

[21] C. A. Balanis, *Antenna Theory Analysis and Design*, Wiley Publishers, New Jersey, USA, 4th edition, 2016.

[22] S. Cruciani, V. D. Santis, M. Feliziani, and F. Maradei, "Cole-Cole vs Debye models for the assessment of electromagnetic fields inside biological tissues produced by wideband EMF sources," in *Proceedings of the IEEE Asia-Pacific Symposium on Electroman. Comp. (APEMC)*, pp. 685–688, Singapore, May 2012.

[23] J. G. Elmore, M. B. Barton, V. M. Moceri, S. Polk, P. J. Arena, and S. W. Fletcher, "Ten-year risk of false positive screening mammograms and clinical breast examinations," *New England Journal of Medicine*, vol. 338, no. 16, pp. 1089–1096, 1998.

[24] Y. Endo, Y. Tezuka, K. Saito, and K. Ito, "Dielectric properties and water contents of coagulated biological tissue by microwave heating," *IEICE Communications Express*, vol. 4, no. 4, pp. 105–110, 2015.

[25] E. C. Fear, X. Li, S. C. Hagness, and M. A. Stuchly, "Confocal microwave imaging for breast cancer detection: localization of tumors in three dimensions," *IEEE Transactions on Biomedical Engineering*, vol. 49, no. 8, pp. 812–822, 2002.

[26] A. I. Iskanderani, I. M. Mehedi, A. J. Aljohani et al., "Artificial intelligence-based digital image steganalysis," *Security and Communication Networks*, vol. 2021, Article ID 9923389, 9 pages, 2021.

[27] N. Gianchandani, A. Jaiswal, D. Singh, V. Kumar, and M. Kaur, "Rapid COVID-19 diagnosis using ensemble deep transfer learning models from chest radiographic images," *Journal of Ambient Intelligence and Humanized Computing*, pp. 1–13, 2020.

[28] D. Singh, V. Kumar, V. Yadav, and M. Kaur, "Deep neural network-based screening model for COVID-19-infected patients using chest X-ray images," *International Journal of Pattern Recognition and Artificial Intelligence*, vol. 35, no. 03, Article ID 2151004, 2021.

[29] D. Singh, V. Kumar, and M. Kaur, "Densely connected convolutional networks-based COVID-19 screening model," *Applied Intelligence*, vol. 51, no. 5, pp. 3044–3051, 2021.

[30] G. T. Herman, *Fundamentals of Computerized Tomography: Image Reconstruction from Projection*, Springer, Berlin, Germany, 2nd edition, 2009.

[31] P. T. Huynh, A. M. Jarolimek, and S. Daye, "The false-negative mammogram," *RadioGraphics*, vol. 18, no. 5, pp. 1137–1154, 1998.

[32] C. Iavazzo, C. Trompoukis, I. Siempos, and M. Falagas, "The breast: from ancient Greek myths to hippocrates and galen," *Reproductive BioMedicine Online*, vol. 19, no. Suppl 2, pp. 51–54, 2009.

[33] W. T. Joines, Y. Zhang, C. Li, and R. L. Jirtle, "The measured electrical properties of normal and malignant human tissues from 50 to 900 MHz," *Medical Physics*, vol. 21, no. 4, pp. 547–550, 1994.

[34] A. I. Iskanderani, I. M. Mehedi, A. J. Aljohani et al., "Artificial intelligence and medical internet of things framework for diagnosis of coronavirus suspected cases," *Journal of Healthcare Engineering*, vol. 2021, Article ID 3277988, 7 pages, 2021.

[35] A. C. Kak and M. Slaney, *Principles of Computerized Tomographic Imaging*, IEEE Press, New York, 1988.

[36] K.-M. Chew, R. Sudirman, N. Seman, and Y. Ching-Yee, *Human Brain Phantom Modeling Based on Relative Permittivity Dielectric Properties*, in *Proceedings of the Biomedical Engineering and Biotechnology (iCBEB)*, pp. 817–820, Macau, China, May 2012.

[37] M. Klemm, I. J. Craddock, J. A. Leendertz, A. Preece, and R. Benjamin, "Radar-based breast cancer detection using a hemispherical antenna array-experimental results," *IEEE Transactions on Antennas and Propagation*, vol. 57, no. 6, pp. 1692–1704, 2009.

[38] M. Kriege, C. T. M. Brekelmans, C. Boetes et al., "Efficacy of MRI and mammography for breast-cancer screening in women with a familial or genetic predisposition," *New England Journal of Medicine*, vol. 351, no. 5, pp. 427–437, 2004.

[39] M. Lazebnik, E. L. Madsen, G. R. Frank, and S. C. Hagness, "Tissue-mimicking phantom materials for narrowband and ultrawideband microwave applications," *Physics in Medicine and Biology*, vol. 50, no. 18, pp. 4245–4258, 2005.

[40] M. Lazebnik, D. Popovic, L. Mccartney et al., "A large-scale study of the ultrawideband microwave dielectric properties of normal, benign and malignant breast tissues obtained from cancer surgeries," *Physics in Medicine and Biology*, vol. 52, pp. 2637–2656, 2017.

[41] X. Li, S. C. Hagness, B. D. Van Veen, and D. van der Weide, "Experimental investigations of microwave imaging via space-time beamforming for breast cancer detection," *IEEE International Microwave Symposium Digest*, vol. 1, pp. 379–382, 2003.

[42] X. Li, S. K. Davis, S. C. Hagness, D. W. vanderWeide, and B. D. VanVeen, "Microwave imaging via space-time beamforming: experimental investigation of tumor detection in multilayer breast phantoms," *IEEE Transactions on Microwave Theory and Techniques*, vol. 52, no. 8, pp. 1856–1865, 2004.

[43] M. Morrow, J. Waters, and E. Morris, "MRI for breast cancer screening, diagnosis, and treatment," *The Lancet*, vol. 378, no. 9805, pp. 1804–1811, 2011.

[44] N. Nikolova, "Microwave imaging for breast cancer," *IEEE Microwave Magazine*, vol. 12, no. 7, pp. 78–94, 2011.

[45] N. Ozmen, R. Dapp, M. Zapf, H. Gemmeke, N. V. Ruiter, and K. W. A. van Dongen, "Comparing different ultrasound imaging methods for breast cancer detection," *IEEE Transactions on Ultrasonics, Ferroelectrics, and Frequency Control*, vol. 62, no. 4, pp. 637–646, 2015.

[46] P. Banerjee, G. Ghosh, and S. K. Biswas, "A simple method to determine the dielectric constant of small-sized medium-loss samples at X-band frequencies," *International Journal of Electromagnetics and Applications*, vol. 1, no. 1, pp. 12–15, 2011.

[47] J. Radon, "On the determination of functions from their integral values along certain manifolds," *IEEE Transactions on Medical Imaging*, vol. 5, no. 4, pp. 170–176, 1986.

[48] J. M. Sill and E. C. Fear, "Tissue sensing adaptive radar for breast cancer detection-experimental investigation of simple tumor models," *IEEE Transactions on Microwave Theory and Techniques*, vol. 53, no. 11, pp. 3312–3319, 2005.

[49] R. A. Smith, D. Saslow, K. Andrews Sawyer et al., "American cancer society guidelines for breast cancer screening: update 2003," *CA: A Cancer Journal for Clinicians, American Cancer Society Guidelines for Breast Cancer Screening, Updated"*. CA: A Cancer J for Clinician, vol. 53, no. 3, pp. 141–169, 2003.

[50] A. J. Surowiec, S. S. Stuchly, J. R. Barr, and A. Swarup, "Dielectric properties of breast carcinoma and the surrounding tissues," *IEEE Transactions on Biomedical Engineering*, vol. 35, no. 4, pp. 257–263, 1988.

[51] A. J. Surowiec, S. S. Stuchly, J. B. Barr, and A. Swarup, "Dielectric properties of breast carcinoma and the surrounding tissues," *IEEE Transactions on Biomedical Engineering*, vol. 35, no. 4, pp. 257–263, 1988.

[52] A. Swarup, S. S. Stuchly, and A Surowiec, "Dielectric properties of mouse MCA1 fibrosarcoma at different stages of development," *Bioelectromagnetics*, vol. 12, no. 1, pp. 1–8, 1991.

[53] N. S Syarifah, M. A Mahmud, Y. K Jusoh, F. Esa, and A. G. E. Sutjipto, "Complex permittivity determination of glycerol using graphical and numerical technique," *Australian Journal of Basic and Applied Sciences*, vol. 11, no. 10, pp. 172–179, 2017.